J. Membrane Biol. 131, 143–149 (1993)

The Journal of
Membrane Biology
© Springer-Verlag New York Inc. 1993

A Patch-Clamp Study of the Ionic Selectivity of the Large Conductance, Ca-Activated Chloride Channel in Muscle Vesicles Prepared from *Ascaris suum*

D.M. Dixon, M. Valkanov†, and R.J. Martin

Department of Pre-Clinical Veterinary Sciences, R.(D).S.V.S., University of Edinburgh, Edinburgh EH9 1QH, and †Central Laboratory of Biophysics, Bulgarian Academy of Sciences, Sofia, Bulgaria

Summary. Plasma membrane vesicles prepared from the bag region of the somatic muscle cell of the parasite *Ascaris suum* contain a large conductance, voltage-sensitive, calcium-activated chloride channel. The ability of this channel to conduct a variety of anions has been investigated using the patch-clamp technique on isolated inside-out patches of muscle membrane. Symmetrical Cl solutions (140 mM) produced single-channel I/V plots with reversal potentials of 0 mV, substitution of bath Cl by 140 mM NO_3, Br and I caused depolarizing shifts in the reversal potentials. Replacement of the internal Cl by F (140 mM) caused a large hyperpolarizing shift in the reversal potential. The channel displayed a permeability sequence of $I > Br = NO_3 > Cl > F$ which differed from the corresponding conductance sequence $Cl > NO_3 = Br = I > F$. The ionic environment within the channel pore has been investigated using Reuter and Stevens (1980) plots to describe the selectivity and "fluidity" of the channel pore. In addition, the approach of Wright and Diamond (1977) was employed to estimate the number of cationic binding sites within the channel pore. The channel is relatively fluid but the number of cationic binding sites varies inversely with the ionic radius of the anion from 2.15 for F to 0.89 for the large planar anion NO_3.

Key Words *Ascaris suum* · chloride channels · calcium · anion channel · ionic permeability

Introduction

Ascaris suum is a large intestinal nematode parasite of the pig which has been developed as a preparation suitable for electrophysiological study (Jarman, 1959; Martin, 1980). The somatic muscle cells of *Ascaris* (Rosenbluth, 1965*a*,*b*; 1967) are divided into three regions: (i) a large balloon-shaped structure containing the nucleus known as the bag, (ii) a contractile spindle region, (iii) a thin process known as the arm that passes from the bag to a nerve cord.

Studies investigating the ionic basis of the resting membrane potential recorded from the bag region of the muscle cell (Del Castillo, DeMellow & Morales, 1964; Brading & Caldwell, 1971) found that the low resting membrane potential, −30 mV, was little affected by extracellular potassium but extracellular chloride had large effects, demonstrating a relatively high chloride permeability. Ion flux experiments (Caldwell & Ellory, 1968) recorded permeability ratios for K, Na and Cl of 1 : 4 : 7, respectively.

Subsequently, single-channel studies on the muscle bag region have shown that there are at least three types of chloride channel present in the membrane. There is a 22 pS GABA-activated channel (Martin, 1985), a 9–15 pS channel which may be activated by the anthelmintic dihydroavermectin (Martin & Pennington, 1989) and a 200 pS high conductance Ca-activated chloride channel (Thorn & Martin, 1987). In this paper we have investigated further the nature of the anion permeability of the high conductance Ca-activated chloride channel with a view to gaining further insight into its function.

Materials and Methods

Preparation of Muscle Vesicles

A. suum were obtained from the local slaughter house and maintained at 37°C in Locke's solution. The Locke's solution was changed daily and the worms were discarded after 4–5 days. A 2 cm section of worm, taken 5 cm below the head region, was cut along one lateral line, the gut removed and the resulting flap pinned out, cuticle side down, onto the base of a Sylgard coated petri dish. The preparation was washed with extracellular solution (concentration in mM): NaCl, 35; Na Acetate, 105; KCl, 2; $MgCl_2$, 2; HEPES, 10; glucose, 3; ascorbic acid, 2; EGTA, 1; pH 7.2 with NaOH. The flap was then incubated for 10 min in enzyme solution (collagenase, 1 mg/ml in EGTA-free extracellular solution). Following enzyme treatment the preparation was thoroughly washed and incubated in extracellular solution at 37°C. Approximately 1

hr after collagenase treatment vesicles could be seen "budding" off the bag region of the muscle cell. These muscle vesicles were easily harvested with a Pasteur pipette and placed into the recording chamber.

Recording Setup

Microelectrodes were pulled from micro-hematocrit capillary glass (Garner Glass 7052) of resistance 1–3 MΩ and coated with Sylgard to improve frequency responses. Single-channel recordings were made from inside-out patches of muscle membrane with seal resistances >1GΩ. The currents were monitored using a List EPC7 current-voltage converter. The signal was filtered by an 8-pole Bessel filter (3 dB, 1 kHz), recorded on computer diskette using an IBM PC2/70 and monitored on an oscilloscope (Tektronix 5113 dual beam). Experiments were carried out using CED Patch Clamp Software in conjunction with a CED 1401 intelligent interface. Using this system, a precise pattern of pulsed stimulation was applied to the patch and recorded directly to disk for analysis. The two protocols used to stimulate channel activity are illustrated below. Voltage sensitivity of the channel openings was illustrated using stimulation protocol 1 while continuous *I/V* plots were obtained using stimulation protocol 2 (*see* Fig. 1). Samples were taken at a rate of 7.5 kHz and currents were averaged over 10 points (i.e., over 1.3 ms) to further reduce noise during estimation of reversal potentials.

Experimental Procedure

Experiments were performed at room temperature (15–22°C). The experimental chamber was mounted on the stage of a Reichert-Jung Biostar inverted microscope and viewed at 200× magnification.

Ion substitution experiments were carried out using a series of fine capillary perfusion tubes supplying various solutions to the recording chamber. Gravity fluid supply provided a steady linear flow of test solutions into which the patch electrode was moved allowing up to five different solutions to be tested on each patch. The pipette solution remained constant throughout all experiments: (in mM) chloride, 140; Mg Acetate, 2; Ca Acetate, 1; HEPES, 10; pH 7.2 with CsOH. The bath solution was: (in mM) test anion, 140; Mg Acetate, 2; Ca Acetate, 1; HEPES, 10; pH 7.2 with CsOH, test anions being either Cl, I, F, Br, or NO_3. Initial recordings for each patch were made between bath and pipette before perfusion was initiated to ascertain whether the mechanical disturbance of the patch by the liquid flow had any effect on channel activity. In addition, each anion was tested both as the bath anion and as a perfused anion to ensure the perfusion procedure had no effect on the ability of the channel to conduct each particular anion. In approximately 10% of patches channel activity would cease when perfusion commenced. This phenomenon was independent of the anion species being perfused; these experiments were discarded, all other recordings were unaffected by the perfusion treatment.

The chamber was grounded using an agar bridge/AgCl electrode. Junction potentials were measured and were negligible <0.2 mV and were subsequently ignored in all calculations.

Analysis

Continuous *I/V* plots were recorded directly onto an IBM PC2/70 for analysis using CED patch-clamp software. Leakage currents were subtracted from *I/V* relationships and both slope conductance and reversal potentials were determined directly from each sweep using cursors provided by the software.

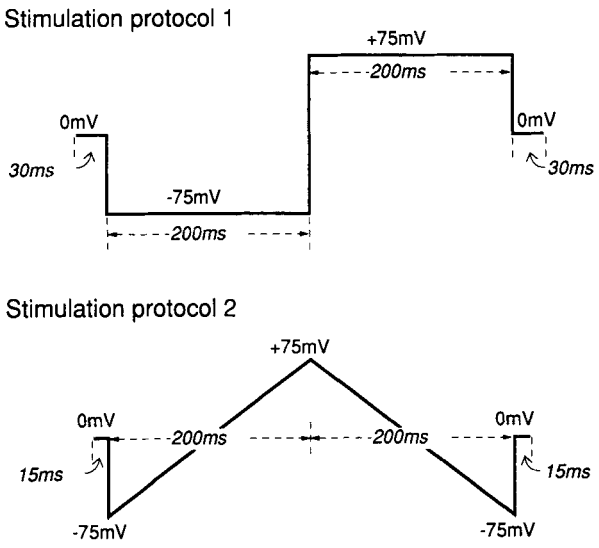

Fig. 1. Diagrammatic representation of the parameters used to stimulate channel activity.

Determination of Permeability Ratios

In ion substitution experiments the Goldman-Hodgkin-Katz equation (Goldman, 1943; Hodgkin & Katz, 1949) was used to calculate the relative permeability P_A/P_{Cl} of anions A^- with respect to Cl^-.

$$Erev = \frac{RT}{F} \ln \frac{[[Cl_i] + P_A/P_{Cl}[A_i]]}{[[Cl_o] + P_A/P_{Cl}[A_o]]} \quad (1)$$

Subscripts *i* and *o* denote internal and external ion species respectively and R, T and F have their usual meanings.

Data Analysis

Results are expressed as mean ± SEM. Significance was tested using unpaired *t*-test. The following *P* values apply to the notation used in the permeability and conductance sequences given in the results section.

=: no significance difference
>: $P < 0.05$
≥: $0.1 < P < 0.05$

Results

All experiments were carried out on vesicles harvested not more than 4 hr before, after which time the quality of the preparation began to decline. Using stimulation protocol 1 (Fig. 1), large amplitude (−14 pA) currents were recorded at the hyperpolarized

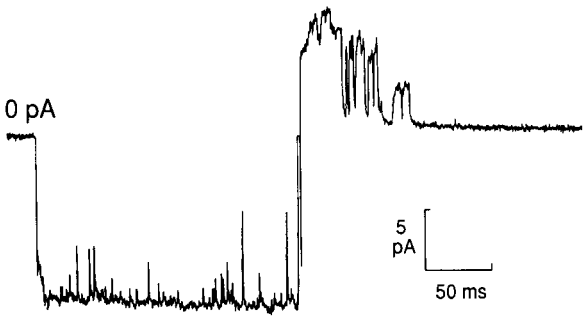

Fig. 2. Voltage dependence of Ca-activated chloride currents obtained from an isolated inside-out patch in symmetrical chloride (140 mM) solution using stimulation protocol 1.

potential of −75 mV (Fig. 2) in symmetrical chloride (140 mM) solution. Upon step depolarization to +75 mV both the current amplitude and the frequency of opening decreased (Fig. 2). In addition substates were seen in many preparations at depolarized potentials (*see* Thorn & Martin, 1987). Consequently, channel conductance was calculated from the linear (hyperpolarized potentials) of the *I/V* relationship.

The calcium-dependent chloride channel in *Ascaris* is selectively permeable to chloride (Thorn & Martin, 1987). All permeability studies in this series of experiments were carried out using the cesium salts of the anions under test. The possible permeability of cesium was assessed using an external (pipette) solution containing 70 mM CsCl, 2 mM $MgCl_2$, 1 mM $CaCl_2$, 10 mM HEPES and an internal (bath) solution containing 140 mM CsCl, 2 mM $MgCl_2$, 1 mM $CaCl_2$, 10 mM HEPES. Assuming the channel only conducts chloride, the reversal potential predicted using the Goldman-Hodgkin-Katz equation [Eq. (1)] is 16.45 mV. The actual reversal potential, measured in two experiments under the ionic conditions described above, was 16.72 mV and 14.5 mV, indicating the cesium permeability of the channel is negligible.

The effect on the conductance and reversal potential of the calcium-activated chloride channel, upon replacing intracellular chloride with the other halides and the anion nitrate, is illustrated in Fig. 3. Symmetrical chloride solution (140 mM) (Fig. 3*A*) affords an *I/V* graph that passes through the origin giving a reversal potential of 0.03 ± 0.47 mV and a slope conductance of 144.3 ± 1.4 pS (Table). Substitution of the bath chloride with Br^-, I^- or NO_3^- (140 mM) causes a depolarizing shift in the *I/V* plot for each ion, thereby producing a positive reversal potential of 3.35 ± 0.66; 8.28 ± 2.06 and 2.87 ± 0.37 mV, respectively (Table). The slope conductance upon substitution of the bath chloride with Br^-, I^- or NO_3^- (140 mM) reduced to 118.8 ± 1.1, 112.6

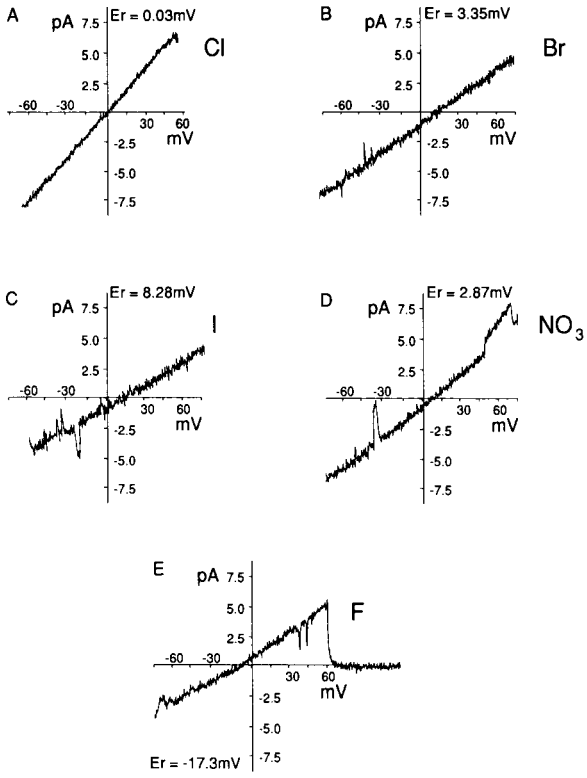

Fig. 3. *I/V* plots from isolated inside-out patches. Pipette solution contains 140 mM chloride the bath solution is varied: (*A*) chloride; (*B*) bromide; (*C*) iodide; (*D*) nitrate and (*E*) fluoride, each at a concentration of 140 mM.

± 1.8 and 128.1 ± 1.1 pS, respectively. However, application of F^- to the inside of the patch results in a hyperpolarizing shift in the *I/V* relationship, affording a negative reversal potential of −17.3 ± 1.99 mV and a reduced conductance of 78.2 ± 1.2 pS. The *I/V* relationships illustrated in Fig. 3 are the result of a single sweep from −75 to +75 mV as produced by stimulation protocol 2. Both Fig. 3*A* and *B* show a single-channel opening for the whole duration of the sweep. The channel can be observed closing during depolarization in Fig. 3*E* and briefly closing and opening again during hyperpolarization in Fig. 3*D*. Also in Fig. 3*D*, in the depolarization quadrant of the *I/V* plot, a second channel opens, thereby producing a portion of the record with a steeper gradient, i.e., larger conductance. This second channel can be seen somewhat briefly in Fig. 3*C* during hyperpolarization.

The reversal potentials were used to calculate the permeability ratios P_A/P_{Cl} of anions A^- relative to Cl^- [Eq. (1), Table]. Figure 4 shows a plot of selectivity isotherms taken from Wright and Diamond (1977), the permeability ratio P_A/P_{Cl} of an anion relative to chloride is plotted on the ordinate with the permeability of I^- relative to Cl^- plotted

Table. Data obtained from isolated inside-out patches

Internal ion (140 mM)	Reversal potential (mV)	P_A/P_{Cl}	Conductance (pS)	nq	Number of patches
Chloride	+0.03 ± 0.47	1.05 ± 0.02	144.3 ± 1.4	1.43	5 (46)
Iodide	+8.28 ± 2.06	1.34 ± 0.11	112.6 ± 1.8	1.65	3 (17)
Bromide	+3.35 ± 0.66	1.16 ± 0.03	118.8 ± 1.1	1.78	3 (17)
Fluoride	−17.3 ± 1.99	0.52 ± 0.04	78.2 ± 1.2	2.15	3 (18)
Nitrate	+2.87 ± 0.37	1.12 ± 0.02	128.1 ± 1.1	0.89	5 (10)

External (pipette) solution contained 140 mM chloride. P_A/P_{Cl} represents the permeability ratio of anion A^- to Cl^-. Numbers in parentheses refer to the total number of *I/V* plots constructed for each anion. nq is number of cationic binding sites within channel pore.

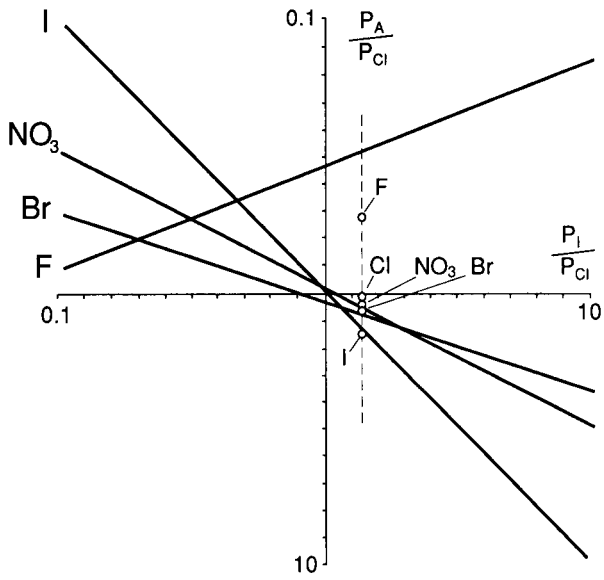

Fig. 4. Selectivity of the Ca-activated chloride channel for the halides and nitrate. Solid lines represent the selectivity isotherms taken from Wright and Diamond (1977). The isotherms represent permeability of the anions observed in a large number of different biological systems. The permeability ratio for each anion relative to chloride (P_A/P_{Cl}) is plotted on the ordinate with the permeability of iodide relative to chloride (P_I/P_{Cl}) on the abscissa. Intersections between the five isotherms represent the transitions among the seven permeability sequences of Wright and Diamond (1977).

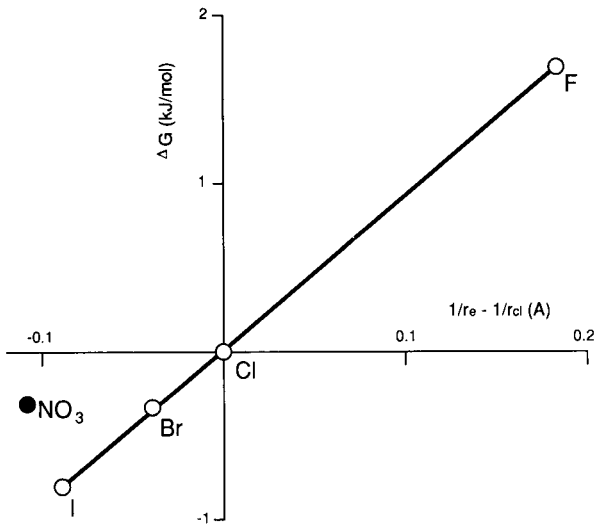

Fig. 5. Reuter and Stevens (1980) plot of free energy barriers for the anions as a function of the reciprocal of anionic radii. The energy difference ΔG for the rate-limiting barrier of each anion, relative to chloride, is plotted on the ordinate and the difference between the inverse of their crystal radii plotted on the abscissa. The line represents a fit with the linear term $a_1 = 9.1$ kJAmol^{-1} in Eq. (6).

on the abscissa. Seven different halide selectivity sequences can be drawn from this graph according to the intersection of the various isotherms. The halide selectivity sequence will vary according to the biological system and channel under test. The Ca-activated chloride channel affords a halide selectivity sequence of I > Br > Cl > F; i.e., sequence 1 of Wright and Diamond (1977). The ion selectivity of a channel is determined by both the ionic environment within the channel pore and by the interaction between the channel wall and ions passing through the channel. Using the extended Eisenman (1961, 1962; Eisenman & Horn, 1983) theory of Wright and Diamond (1977) the number of cationic binding sites within the channel can be estimated. Hydrated anions entering the channel are transferred from water to cationic sites in the channel wall. The ease with which an anion passes through the channel is therefore dependent on the difference between the anion hydration energy (ΔG_H) and the field strength of the cationic binding site (ΔG_{site}). The energy required to transfer 1 mol of anion from water to channel binding site is (Wright & Diamond, 1977)

$$\Delta G_{trans} = \Delta G_{site} - \Delta G_H \quad (2)$$

Assuming channel walls have fixed monopolar posi-

tively charged sites of radius, r with point positive charge q_+ the principal ion-site interaction can be represented by the term $nq_+q_-/(r_+ + r_-)$ where r_+ and r_- are the ionic radius (Å) of cationic monopoles comprising each site and touching each anion. Then taking q_- as -1 for all monovalent anions, assigning the appropriate proportionality constant for the usual units, and assuming the positively charged sites within channel walls consist of $-NH_3^+$, $>NH_2^+$, NH^+, N^+, residues, then r_+ can be taken as the radius of nitrogen, 1.5 Å

$$\Delta G_{\text{site}} = -1388nq_+/(r_- + r_+) \tag{3}$$

Using Pauling ionic radii and appropriate hydration energies (Wright & Diamond, 1977) the number of positive charges, nq, within the channel can be evaluated by

$$\Delta G = \Delta G_{\text{trans}}(A^-) - \Delta G_{\text{trans}}(Cl^-) \tag{4}$$

ΔG of anion A^- and Cl^- can be expressed in terms of the permeability ratio of anion A^- to Cl^- (Borman, Hamill & Sakmann, 1987)

$$\Delta G = RT \ln P_A/P_{Cl} \tag{5}$$

The number of positive charges within the channel that are in contact with the anion can therefore be calculated from the permeability ratios given in the Table. It can be seen from the Table that the values of nq vary widely from a low of 0.89 for NO_3 to a high of 2.15 for F.

Another explanation of the anion selectivity can be drawn from the theory of Reuter and Stevens (1980), which relates the "fluidity" of the channel to that of free water. Assuming the interaction between anion and water is entirely electrostatic (Buckingham, 1957), then the quantity influencing the anionic permeability would be the electric field around the anion, i.e., its radius and valence. In the case of a channel with only one rate-limiting barrier, the barrier height G will depend on the inverse of the ionic radius of the anion. This can be represented as a power series where the energy function G has been expanded about the reciprocal radius of Cl^- as the reference ion

$$G(1/r_A) = G(1/r_{Cl}) + a_1(1/r_A - 1/r_{Cl}) + a_2(1/r_A - 1/r_{Cl})^2 \tag{6}$$

This equation is related to relative permeabilities expressed in Eq. (5). Incorporating Eq. (5) into Eq. (6) affords

$$\Delta G = G(1/r_A) - G(1/r_{Cl}) = \frac{RT}{F} \ln \frac{P_{Cl}}{P_A} \tag{7}$$

Therefore, plotting ΔG as a function of $1/r_A - 1/r_{Cl}$ affords a physical interpretation of the coefficients of expansion (a_1). When the relationship is linear the coefficient a_1 can be used to indicate the "fluidity" of the channel water structure as compared to free water (Reuter & Stevens, 1980), and therefore gives an indication of the constraints placed on the diffusion of ions through the channel; this is illustrated in Fig. 5. In the *Ascaris* calcium-dependent chloride channel the halide anions afford a straight line that can be described by the linear portion of Eq. (6) with a coefficient a_1 of 9.1 kJÅmol^{-1}. NO_3 does not fit the linear function of the power Eq. (6), ΔG in this case is more positive than that predicted for an ion of its radius.

Discussion

As shown in a previous study (Thorn & Martin, 1987), the activity of the calcium-activated chloride channel of *A. suum* decreases upon depolarization. The profile of voltage dependence of this calcium-activated Cl channel differs from that found in other large conductance chloride channels which tend to be active only in the range ±30 mV about zero (Grey, Bevan & Ritchie, 1984; Young et al., 1984). Whereas the calcium-dependent Cl current in *Ascaris* remains active at potentials in excess of −150 mV (*data not shown*) and only rectifies at positive membrane potentials.

The channel is not especially selective between the anions tested in this paper. The permeability ratios of halides follow sequence 1 of Wright and Diamond (1977), namely I > Br > Cl > F, indicative of a low field strength cationic binding site. Selectivity sequence 1 is displayed by several large conductance Cl channels (Grey et al., 1984; Marty, Tan & Trautmann, 1984; Young et al., 1984). In addition, the halide selectivity sequence of the smaller (30 pS) chloride channel in rat hippocampal neurons (Franciolini & Nonner, 1987) also conformed to sequence 1. However, unlike the calcium-activated chloride channel in *Ascaris*, the small conductance chloride channel was more permeable to nitrate than iodide. This halide permeability sequence is in agreement with that measured for the whole muscle membrane (Del Castillo et al., 1964) using changes in *Ascaris* resting membrane potential upon substitution of anions for external chloride. This method afforded a halide permeability sequence of I > Br > Cl; however, NO_3 was found to be more permeable

than I. Using a similar methology Rheinhallt Parri et al. (1991) investigated the selectivity of the GABA operated channel of the somatic muscle cell of *Ascaris*. Unfortunately, large standard errors prevented full resolution of the data; however, NO_3, I and Br were all more permeable than Cl. Likewise a similar permeability sequence ($I > NO_3 > Br > Cl > F$) is displayed by a calcium-dependent chloride current in isolated cells from rat lacrimal glands (Evans & Marty, 1986).

It would appear that the calcium-dependent chloride channel of *Ascaris* is not simply a water-filled pore as the conduction sequence differs from the permeability sequence, a feature usually indicative of a binding site for permeant ions within the channel wall. In addition, Fig. 5 illustrates ΔG [Eq. (7)] plotted as a function of the reciprocal of ion size. The data for the halides are described by the linear term in Eq. (6); a simple linear relationship between ion size and ΔG usually indicates a nonselective channel pore (Reuter & Stevens, 1980). The linear term a_1 is 9.1 kJÅmol^{-1}, for the calcium-dependent chloride channel, a_1 being a measure of the "fluidity" of the channel water structure as compared to free water (Reuter & Stevens, 1980). Thus, the calcium-dependent chloride channel is relatively "fluid." However, stronger constraints are placed on the diffusion of water molecules in the calcium-dependent chloride channel compared to water diffusion in the acetylcholine receptor channel, in whose case a_1 is only 1.4 kJÅmol^{-1}, indicating a very "fluid" channel. However, GABA and glycine gated chloride channels in mouse cultured spinal neurones are less "fluid." Both channels place stronger constraints on the diffusion of water, affording a_1 values of 28.8 and 18.8 kJÅmol^{-1}, respectively (Bormann, Hamill & Sakmann 1987).

However, ΔG_{NO_3} is not described by the linear portion of Eq. (6). ΔG for NO_3 is more positive than expected for an ion of its radius. This would suggest NO_3 interacts with water more strongly than anticipated. However, this is not borne out by the low hydration energy ΔG_H of NO_3 (Wright & Diamond, 1977). Therefore, ΔG for NO_3 is perhaps more influenced by ΔG_{site} than the halides. In calculating ΔG several assumptions are made, the most important being that the anions are spherical and as such the electrostatic interaction between water, anion and their surroundings will depend on the inverse of the ionic radius of the anion (Wright & Diamond, 1977). This is clearly not the case for NO_3 which is a planar molecule (Pauling, 1960). The radius of the horizontal plane of the NO_3 would therefore be an overestimation of the radius of NO_3 if the molecule interacts with the channel cationic binding sites along the vertical plane. Such a reduction in radius would shift ΔG_{NO_3} to the right in Fig. 5 bringing it in line with the halides. This hypothesis is borne out by the estimation of nq, the number of cationic binding sites within the channel with which the anions interact. Two simple interpretations of these data can be offered. The first would be to suggest that certain binding sites are inaccessible to larger anions such as nitrate. The second interpretation takes into account the possibility of an anion of small ionic radius and, therefore, dense negative charge to induce dipole moments within the channel wall, thereby 'creating' additional binding sites as it passes through the channel pore.

The role of this channel remains open to question. The channel is active at -30 mV, the resting membrane potential (RMP) of the somatic muscle cell of *Ascaris*, (Del Castillo, 1964; Brading & Caldwell, 1971) and could therefore contribute to the maintenance of the RMP. The chloride concentration of the perienteric fluid within the body cavity of *A. suum* is maintained at a lower concentration (52 mM) than that of the surrounding environment (Hobson, Stephenson & Eden, 1952). Hobson et al. (1952) also demonstrated that chloride is transported across the body wall to the outside and that the active site of this transport is a feature of the muscle or hypodermis. A possible role for the calcium-dependent chloride current in *Ascaris* is, therefore, the transport of chloride across the bag region of the muscle cell. In addition, preliminary experiments conducted within our laboratory indicate that the channel is able to conduct organic acids that form the products of anaerobic respiration. A possible further role of this channel, therefore, is the removal of metabolic waste products from the muscle cell.

This work was supported by the Scientific & Engineering Research Council (S.E.R.C.).

References

Borman, J., Hamill, O.P., Sakmann, B. 1987. Mechanism of anion permeation through channels gated by glycine and γ-aminobutyric acid in mouse cultured spinal neurons. *J. Physiol.* **385**:243–286

Brading, A.F., Caldwell, P.C. 1971. The resting membrane potential of somatic muscle cells of *Ascaris lumbricoides*. *J. Physiol.* **27**:605–624

Buckingham, A.D. 1957. A theory of ion-solvent interaction. *Disc. of the Faraday Soc.* **24**:151–157

Caldwell, P.C., Ellory, J.C. 1968. Ion movements in somatic muscle cells of *Ascaris lumbricoides*. *J. Physiol.* **197**:75–76P

Del Castillo, J., DeMellow, W.C., Morales, T. 1964. Influence of some ions on the membrane potential of *Ascaris* muscle. *J. Gen. Physiol.* **48**:129–140

Eisenman, G. 1961. On elementary atomic origin of equilibrium

ionic specificity. *In*: Symposium on Membrane Transport and Metabolism. A. Kleinzeller and A. Kotyk, editors. pp. 163–179. Academic, New York

Eisenman, G. 1962. Cation selective glass electrodes and their mode of operation. *Biophys. J.* **2**:259–323

Eisenman, G., Horn, R. 1983. Ionic selectivity revisited: the role of kinetic and equilibrium processes in ion permeation through channels. *J. Membrane Biol.* **76**:197–225

Evans, M.G., Marty, A. 1986. Calcium-dependent chloride currents in isolated cells from rat lacrimal glands. *J. Physiol.* **378**:437–460

Franciolini, F., Nonner, W. 1987. Anion and cation permeability of a chloride channel in rat hippocampal neurons. *J. Gen. Physiol.* **90**:453–478

Goldman, D.E. 1943. Potential impedence and rectification in membranes. *J. Gen. Physiol.* **27**:37–60

Grey, P.T.A., Bevan, S., Ritchie, J.M. 1984. High conductance anion-selective channels in rat cultivated Schwann cells. *Proc. R. Soc. London B.* **221**:395–409

Hobson, A.D., Stephenson, W., Eden, A. 1952. Studies on the physiology of *Ascaris lumbricoides*. 2. The inorganic composition of the body fluid in relation to that of the external environment. *J. Exp. Biol.* **29**:22–29

Hodgkin, A.L., Katz, B. 1949. The effect of sodium ions on the electrical activity of the giant axion of the squid. *J. Physiol.* **108**:37–77

Jarman, M. 1959. Electric activity in muscle cells of *Ascaris* muscle. *Nature* **184**:1244

Martin, R.J. 1980. The effect of GABA on the input conductance and membrane potential of *Ascaris* muscle. *Br. J. Pharmacol.* **71**:99–106

Martin, R.J. 1985. GABA and piperazine-activated single channel currents from *A. suum*. *J. Physiol.* **354**:46P

Martin, R.J., Pennington, A.J. 1989. A patch-clamp study of dihydroavermectin on *Ascaris* muscle. *Br. J. Pharmacol.* **98**:747–756

Marty, A., Tan, Y.P., Trautmann, A. 1984. Three types of calcium-dependent channels in rat lacrimal glands. *J. Physiol.* **377**:293–325

Pauling, L. 1960. The Nature of the Chemical Bond. pp. 283–284. Cornell University, New York

Reuter, H. Stevens, C.F. 1980. Ion conductance and ion selectivity of potassium channels in snail neurones. *J. Membrane Biol.* **57**:103–118

Rheinallt Parri, H., Holden-Dye, L., Walker, R.J. 1991. Studies on the ionic selectivity of the GABA-operated chloride on the somatic muscle bag cells of the parasitic nematode *Ascaris suum*. *Exp. Physiol.* **76**:597–606

Rosenbluth, J. 1965*a*. Ultrastructural organisation of obliquely striated muscle fibres in *Ascaris lumbricoides*. *J. Cell Biol.* **25**:494–515

Rosenbluth, J. 1965*b*. Ultrastructure of somatic muscle cells in *Ascaris lumbricoides*. II. Intermuscular junctions, neuromuscular junctions, and glycogen stores. *J. Cell Biol.* **26**:579–591

Rosenbluth, J. 1967. Obliquely striated muscle. III. Contraction mechanism of *Ascaris* body muscle. *J. Cell Biol.* **34**:15–33

Thorn, P., Martin, R.J. 1987. A high conductance calcium-dependent chloride channel in *A. suum* muscle. *J. Exp. Physiol.* **72**:31–49

Wright, E.M., Diamond, J.M. 1977. Anion selectivity in biological systems. *Physiol. Rev.* **57**:109–156

Young, G.P.H., Young, J.D.E., Destipande, A.K., Goldstein, M., Koide, S.S., Cohn, Z.A. 1984. A Ca^{2+}-activated channel from *Xenopus laevis* oocyte membranes reconstituted into planar bilayers. *Proc. Natl. Acad. Sci. USA* **81**:5155–5159

Received 29 April 1992; revised 19 August 1992